Talanta 115 (2013) 911–919

Contents lists available at SciVerse ScienceDirect

Talanta

journal homepage: www.elsevier.com/locate/talanta

Analytical application of polymethylene blue-multiwalled carbon nanotubes modified glassy carbon electrode on anticancer drug irinotecan and determination of its ionization constant value

Nurgul Karadas [a,b], Senem Sanli [c], Bediha Akmese [b], Burcu Dogan-Topal [a], Alp Can [d], Sibel A. Ozkan [a,*]

[a] Faculty of Pharmacy, Department of Analytical Chemistry, Ankara University, 06100 Ankara, Turkey
[b] Faculty of Science and Arts, Department of Chemistry, Hitit University, Corum, Turkey
[c] Faculty of Science and Arts, Department of Chemistry, Usak University, Usak, Turkey
[d] Faculty of Medicine, Department of Histology and Embryology, Ankara University, Ankara, Turkey

ARTICLE INFO

Article history:
Received 5 April 2013
Received in revised form
3 July 2013
Accepted 4 July 2013
Available online 13 July 2013

Keywords:
Carbon nanotubes
Irinotecan
Poly (methylene blue)
Ionization constant
Reversed-phase liquid chromatography

ABSTRACT

The voltammetric behavior of anticancer drug irinotecan (IRT) was investigated at poly (methylene blue)/multi-walled carbon nanotube (PMB/MWCNT) modified glassy carbon electrode (GCE). The modified electrode surface was characterized by a scanning electron microscope (SEM). The PMB/MWCNT modified GCE exhibits a distinct shift of the oxidation potential of IRT on the cathodic direction and a considerable enhancement of the peak current compared with bare electrode. The calibration curve was linear between the concentration range 8.0×10^{-6} and 8.0×10^{-5} M with the detection limit of 2.14×10^{-7} M by differential pulse voltammetry in pH 10.0 Britton–Robinson buffer solution. Controlled potential coulometry was applied to find transferred electron numbers due to the oxidation of IRT. In this study, the pK_a value of IRT was also determined by the dependence of the retention factor on the pH of the mobile phase. The effect of the mobile phase composition on the ionization constant was studied by measuring the pK_a at different acetonitrile–water mixtures, ranging between 35 and 50% (v/v) using the reversed-phase liquid chromatography (RP-LC) method with UV detector. IRT was exposed to thermal, photolytic, hydrolytic and oxidative stress conditions, and the stressed samples were detected by the proposed method. Sensitive, rapid, and fully validated electrochemical and RP-LC methods for the determination of IRT in its dosage form were presented in details.

1. Introduction

Irinotecan HCl (Scheme 1) is a new drug, which has antitumor activity in a wide range of malignancies, such as metastatic colorectal cancer, upper gastrointestinal, pancreatic, lung, breast cancer, and gynecological malignancies [1,2]. IRT is a potent inhibitor of topoisomerase I. In chemical terms, it is a semisynthetic analouge of the natural alkoloid camptothecin. IRT is activated by hydrolysis of SN-38 (7-ethly-10-hydroxy-camptothecin) as an inhibitor of topoisomerase I. The inhibition of topoisomerase I by the active metabolite SN-38 eventually leads to inhibition of both DNA replication and transcription.

Few analytical procedures have been described for the determination of IRT including reduction behavior at the hanging mercury drop electrode by cyclic voltammetry [3] and liquid chromatography methods [4–9]. Because of their selectivity, sensitivity, and overall versatility, the development of reliable and validated reversed-phase liquid chromatography (RP-LC) methods have received considerable attention in the quality control of drugs and quantitative determination in their dosage forms.

Most pharmacologically active molecules contain one or more ionizing groups and it is well-known that knowledge of the ionization state of a drug, indicated by the pK_a value, is critical for understanding many properties with respect to pH. The study of acid–base behavior of analytes in binary organic–water solvent systems can be a key in predicting influence of pH on electroanalytical characteristics of drugs. No method has been published in the scientific literature so far for the determination of pK_a values of IRT by electroanalytical and RP-LC methods. The determination of pK_a values by RP-LC is based on the relationships between the capacity factors and the pH values of the mobile phase [10–13]. This technique is also used for determination of dissociation constants since no big quantities of compounds are required for analysis. Moreover, studied samples do not need to be pure and

* Tel./Fax: +90 312 2238243.
E-mail address: ozkan@pharmacy.ankara.edu.tr (S.A. Ozkan).

0039-9140/$ - see front matter © 2013 Elsevier B.V. All rights reserved.
http://dx.doi.org/10.1016/j.talanta.2013.07.006

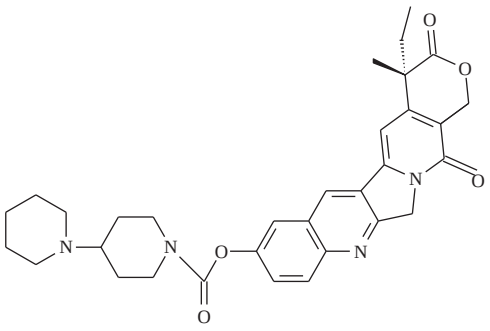

Scheme 1. Chemical structure of IRT.

poor water solubility is not a serious drawback when RP-LC is utilized for this application. No method has been published in the scientific literature so far for the determination of pK_a values of IRT by RP-LC methods. Aqueous pK_a values ($^{w}_{w}$pK_a) of the drug were calculated from the mobile phase pK_a values ($^{s}_{s}$pK_a) determined in different acetonitrile (ACN)–water mixtures by means of the Yasuda–Shedlovsky equation [14] and linear relations between the mole fraction of ACN and the $^{s}_{s}$p$K_a$values. The results of these methods obtained from $^{w}_{w}$pK_a values can be compared with Advanced Chemistry Development, Inc. (ACD/Labs) [15].

Electrochemical methods have been used for the determination of electroactive species in pharmaceuticals and body fluids due to their simplicity and low cost. Only one article has been published on the reduction behavior and dsDNA (double stranded deoxyribonucleic acid) interaction of IRT at the hanging mercury electrode by cyclic voltammetry [3]. The interest in developing electrochemical-sensing devices for use in clinical assay, process control and environmental monitoring is growing rapidly. Carbon nanotubes (CNTs) have been widely used for the development of chemically modified electrodes providing good conductivity, high chemical stability, high surface area and resistance to surface fouling. The electronic properties suggest that CNTs have capability to promote electron transfer reactions and enhanced electrocatalytic activity in electrochemistry. The enhancement of electrocatalytic activity could be explained by the decrease of the overpotential [16]. Thus, they are widely used as electrode materials for tailoring a great variety of electrochemical sensors and biosensors [17–24].

Electropolymerization is a powerful method in targeting selective modification of carbon-based electrodes. The important advantages of electropolymerization are the easy deposition of desired electroactive polymers onto the conductive surface from monomer solutions and the precise electrochemical control of their formation rate and thickness. Electroactive polymers have useful properties such as electronic and ionic conductivity. The conjugated polymers for sensor devices have exhibited an interesting enhancement in the electrocatalytic activity in electrochemistry [25]. Azine-conjugated polymers, such as phenazines, phenothiazines, phenoxazines have been widely used in bioelectrochemistry as redox indicators and mediators [26]. The report revealed that methylene blue (MB) may be polymerized to in neutral aqueous solutions [27].

In recent years, the combination of electroactive polymers and carbon nanotubes matrices received considerable attraction for detection and determination of drugs in electrochemistry. Studies showed that the preparation of composite films composed of both CNTs and conjugated polymers helped to improve matrix properties such as high sensitivity and good stability [28–30].

As yet, there has been no report for the electrooxidative behavior and redox properties of IRT on neither bare nor modified electrodes. In this study, GCE was modified with MWCNT and PMB. The proposed differential pulse voltammetric method was used for the determination of IRT in its pharmaceutical dosage form with MWCNT/PMB modified GCE. Additionally, the pK_a value of IRT is determined in 35, 40, 45, and 50% (v/v) acetonitrile (ACN)–water mixtures. Hence, the fully validated determination methods of IRT were developed and applied to its commercial dosage forms. The stability tests were also performed as per International Conference on Harmonization (ICH) guidelines [31].

2. Experimental

2.1. Reagents

Irinotecan HCl was purchased from Sigma Chemical Co. (St. Louis, MO, U.S.A.) and its pharmaceutical dosage form Tekamen® by Mustafa Nevzat Pharm. Ind. (Istanbul, Turkey). Each sterile apyrogene vial contains 100 mg of irinotecan hydrochloride trihydrate, 225 mg D-sorbitol and 4.5 mg lactic acid in 5 mL solution. The pH of the solution has been adjusted to 3.5 with sodium hydroxide. For electrochemical study, carboxylate functionalized multi-walled carbon nanotubes (I.D × length: 10 × 1.5 μm) were purchased from DropSens. Methylene blue was purchased from Sigma-Aldrich. Buffer solution from sodium dihydrogen phosphate and disodium hydrogen phosphate (Riedel-de-Haen, Germany), ionic strength 0.1 M with pH value 7.0 was used for the electropolymerization of MB and as supporting electrolyte. In these experiments, 0.1 M phosphate buffer solution (PBS) was used for the preparation of pH 6.0–8.0. Also, 0.04 M Britton–Robinson (BR) buffer solution for the 9.0–11.0 pH range. Aqueous solutions were prepared using bi-distilled water. The stock solutions of IRT (1.0×10^{-3} M) were prepared in bi-distilled water and stored at +4 °C. The working solutions of IRT were freshly prepared with supporting electrolyte before measurements.

For the RP-LC method, LC grade acetonitrile (Merck, Darmstadt, Germany) was used as an organic modifier. Sodium hydroxide (Merck, Darmstadt, Germany) and o-phosphoric acid (Riedel-de Haen, Germany) were used for pH adjustment. Several internal standards were tested such as doxorubicin, daunorobicin, quinapril, cilazapril, fenticonazole and tinidazole. Tinidazole was chosen as the internal standard (IS) because of its shorter retention time with better peak shape and better resolution compared to other potential ISs. Standard stock solutions of IRT and IS were prepared in acetonitrile at a concentration of 1.0×10^{-3} M and working solutions were prepared by the dilution using mobile phase. The concentration of IRT for RP-LC studies was varied between the range of 8.02×10^{-7} and 1.93×10^{-5} M. The concentration of IS was maintained at a constant level at 8.09×10^{-6} M. The calibration curve for the RP-LC analysis was constructed by plotting of peak area ratio of the drug to IS versus drug concentration.

The ruggedness and precision of both methods were checked at the same day ($n=5$) and consecutive days ($n=5$) and reported as relative standard deviations (RSD) [32,33]. The accuracy and precision of the developed methods were described in a quantitative fashion by the use of Bias % (relative error).

2.2. Apparatus

All electrochemical studies were performed with using a computer-controlled Autolab potentiostat/galvanostat PGSTAT 302 with GPES 4.9 software. An electrochemical cell with a three-electrode configuration was used with a counter electrode as platinum wire, a glassy carbon working electrode (GCE) (unmodified and/or modified) (Bioanalytical Systems, West Lafayette, IN, USA; Ø: 3 mm, diameter) and saturated Ag/AgCl as reference electrode. pH measurements were carried out using a model 538

pH-meter (WTW, Weilheim, Germany) with an accuracy of ±0.05 pH. DPV conditions were given as follows: pulse amplitude, 50 mV; pulse width 50 ms; scan rate 20 mV s^{-1}. Coulometric measurements were performed with large surface area platinum foil as working electrode in an electrochemical cell using Autolab Potentiostat/Galvanostat PGSTAT 302 with GPES 4.9.

The LC analysis was carried out on a Shimadzu RP-LC system with a pump (LC-20 AD), a DAD detector system (SPD-M 20 A) and column oven (CTO 20 AC). This equipment has a degasser system (DGU 20 A). The system operates at 220 nm for IRT. A Gemini C18 column (4.6 × 250 mm^2, 5 μm) was used as stationary phase at 25 °C. Mettler Toledo MA 235 pH/ion analyzer with Hanna HI 1332 Ag/AgCl combined glass electrode was used for pH measurements.

2.3. Pretreatment of GCE

Electrode pretreatment is an important step to get reproducible results so that GCE was pretreated by two different methods depending on the experiment: (a) mechanical polishing with a smooth polish pad which has 0.01 μm aluminum oxide (BAS velvet polishing pad), and (b) electrochemical treatment by applying cyclic voltammetry between −0.4 V and 1.2 V with 2 consecutive cycles in selected supporting electrolytes.

2.4. Preparation of the PMB/MWCNT modified GCE

One mg (–COOH) functionalized MWCNT was dispersed in 1.0 mL of dimethylformamide (DMF) solvent under ultrasonic agitation for 2 h prior to use. MWCNT in the amounts between 2.5 μL and 15 μL were studied for the optimization of casting of MWCNT on the electrode surface. The optimum amount of CNT was 10 μL. By using micropipets, 10 μL of the dispersed CNT was dropped on the electrode surface followed by heating the electrode in oven at 50 °C for 15 min. The MWCNT modified GCE was kept in room temperature for 1 h. The electro-deposition of the 0.1 mM MB layer on the surface of MWCNT modified GCE in 0.1 M PBS (pH 7.0) by potential cycling between −0.4 V and 1.2 V (versus Ag/AgCl) at a scan rate of 100 mV s^{-1} with 15 cycles. After the electropolymerization procedure, the modified electrode was rinsed in bi-distilled water to remove impurities and used as PMB/MWCNT-modified GCE.

For the cleaning of modified electrode, cyclic voltammetry method was used between each measurement by applying cyclic voltammetry between −0.4 V and 1.2 V with 2 consecutive cycles in the selected supporting electrolytes.

2.5. Chromatographic procedure

Throughout the entire procedure, the effect of solvent composition on the chromatographic separation was investigated at four different solvent levels (35, 40, 45, 50%, v/v). The pH of the mobile phase containing 20 mM phosphoric acid was adjusted between 3.0 and 10.5 by the addition of sodium hydroxide. The flow rate of the mobile phase was 1 mL min^{-1} and injection volume was 20 μL. The retention times (t_R) were determined from three separate injections for each mobile phase composition and pH values. Retention factors for each compound and mobile phase were calculated using the expression $k=(t_R-t_0)/t_0$. The dead time (t_0) was measured by injecting uracil solution (Sigma, USA, 0.1%, in water), which was established for each mobile phase composition and pH studied.

IRT is weak monoprotic base and the ionization process can be expressed as

$$BH^+ \overset{K_a}{\rightleftarrows} B + H^+ \quad (1)$$

The observed retention factors can be described as a function of retention factors of the neutral and ionized species and the equation can be given as

$$k_{obs} = \frac{k_0 + k_1([H^+]/K_a)}{1 + ([H^+]/K_a)} \quad (2)$$

where k_0 and k_1 are the retention factors of the neutral and fully ionized base, respectively.

The pK_a values of studied compounds were determined from k/pH data pairs by means of the non-linear regression program NLREG [34]. This is a general purpose program, where the function to be minimized and the parameters to be estimated can be defined by means of the built-in program editor.

2.6. Procedure for forced degradation study

Degradation studies were attempted for stress conditions of UV light, acid–base, oxidation and heat in oven to evaluate the ability of the proposed method to detect IRT from its degradation product [31].

For hydrolytic and oxidative degradation, solutions were prepared by dissolving drug in ACN and later diluted with hydrochloric acid, sodium hydroxide or hydrogen peroxide solution, to achieve a concentration of 1.61×10^{-4} M of IRT for each solution.

Acid and alkaline hydrolysis of drug substance in solution state was conducted with 1.0 M HCl and 1.0 M NaOH at 80 °C for 30 min. For oxidative stress, sample solutions of drug substance and drug product in 3% hydrogen peroxide were kept at 75 °C for 30 min.

Thermal and photo-degradation of drug substance was carried out in solid state. After the degradation, stock solutions were prepared by dissolving in ACN to achieve a concentration of 1.61×10^{-4} M.

For thermal stress, IRT was placed in a controlled-temperature oven at 100 °C for 6 h.

For photolytic stress, drug sample, in solid state, was irradiated with UV radiation having peak intensities at 254 nm.

2.7. Injectable dosage form assay process and recovery studies

For voltammetric analysis, 1.69 mL Tekamen® (containing 100 mg/5 mL IRT) transferred to a 50 mL of calibrated flask, and completed to the volume with bi-distilled water for voltammetric analysis and with acetonitrile for RP-LC studies. The concentration of the prepared solution is equivalent to 1.0×10^{-3} M. Appropriate solutions were prepared by the dilution of the aliquots of this solution with the selected supporting electrolyte for the voltammetric analysis. The nominal content of the injectable amounts were calculated from the corresponding regression equations of previously plotted calibration plots.

For RP-LC studies, an appropriate volume of injectable dosage form was used to prepare a stock solution in mobile phase at a concentration of 3.21×10^{-4} M and the content of the flask was sonicated for 15 min. This solution was filtered and the filtrate was collected in a clean flask. Appropriate solutions were prepared by taking suitable aliquots of clear filtrate and adding the appropriate IS solution.

To verify the accuracy and reproducibility of the methods and to determine whether the excipients show any interference used in formulations, recovery experiments were carried out [32,35–37]. For this purpose, a certain amount of pure IRT was added to the pre-analyzed injectable dosage form of IRT (and at a constant level of IS for the RP-LC method). The mixtures were analyzed by the DPV and LC-UV. The recovery results were obtained by using the related calibration equations for these techniques for five repeated measurements.

3. Results and discussion

3.1. Electrochemical behavior of IRT at the modified electrodes

A previously published study mentioned the reduction behavior of IRT at the hanging mercury drop electrode by cyclic voltammetry [3]. In our study, the electrooxidation behavior of IRT was investigated on PMB/MWCNT-modified GCE electrode using cyclic voltammetry (CV) and differential pulse voltammetry (DPV). The pH of the supporting electrolyte has a major impact for oxidation of IRT on modified GCE. The pH dependency was studied in 0.1 M phosphate and 0.04 M BR buffers at different pH values between pH 6.0 and 11.0 by DPV. PMB films were unstable in acidic media lower than pH 6.0. IRT molecule, on the other hand, decomposes at pH < 3.0 and pH > 11.0 media. Fig. 1(b) shows the consecutive cyclic voltammograms for the electropolymerization of MB at MWCNT-modified GCE in 0.1 M PBS (pH 7.0) containing 0.1 mM MB for 15 cycles. The potentials were swept between −0.4 and 1.2 V by scanning in the positive direction at a scan rate of 100 mV s^{-1}. There is likely a polymer structure formation as inferred in the Ref. [38].

The anodic behavior of IRT was investigated using CV (Fig. 1a) and DPV techniques in different pH values. To identify the responsible group of the oxidation steps, the oxidation of IRT was compared with some model compounds in published studies related with the pyridine moiety in the quinoline ring and piperidyl rings. Both, pyridine moiety in the quinoline ring and piperidyl group of the molecule may be responsible of the electrooxidation response of IRT. In previous reports, the piperidyl ring was oxidized at about 1.0 V on glassy carbon electrode [39], and the pyridine ring was oxidized at about 0.8 V [40,41]. Literature results showed that the pyridine moiety in the quinoline ring is easily oxidizable than piperidyl ring. In our study, IRT gave only one anodic peak at about 0.6 V at pH 10.0. The piperidyl oxidation peak may not be obtained within the working potential range. Thus, our oxidation peak might belong to a nitrogen atom on the pyridine moiety in the quinoline ring, which has an unpaired electron over the delocalized aromatic system [42]. The evolution of peak potential with pH shows one linear segment. The intersection point of the curves (~pH 9.0) is close to the pK_a value of IRT, and it can be explained by changes in protonation of the acid–base functions in the pyridine moiety in the quinoline ring. This result also strongly proved that the oxidation step of IRT is located on the pyridine moiety in the quinoline ring and attributed to the oxidation of tertiary nitrogen [42,43].

The effect of pH on the peak potential and peak current of IRT were investigated at a pH range of 6.0–11.0 using both CV and DPV methods. Both techniques showed that the peak potential of IRT shifted towards less positive values, indicating proton participation in the oxidation process moved to less positive potentials, with increasing pH. Anodic peak potentials showed a linear dependence on pH with a negative slope of −56.97 mV/pH using DPV technique (Fig. 2a).

$$Ep\ (mV) = 1189 - 56.97\ pH\ (r = 0.977)$$

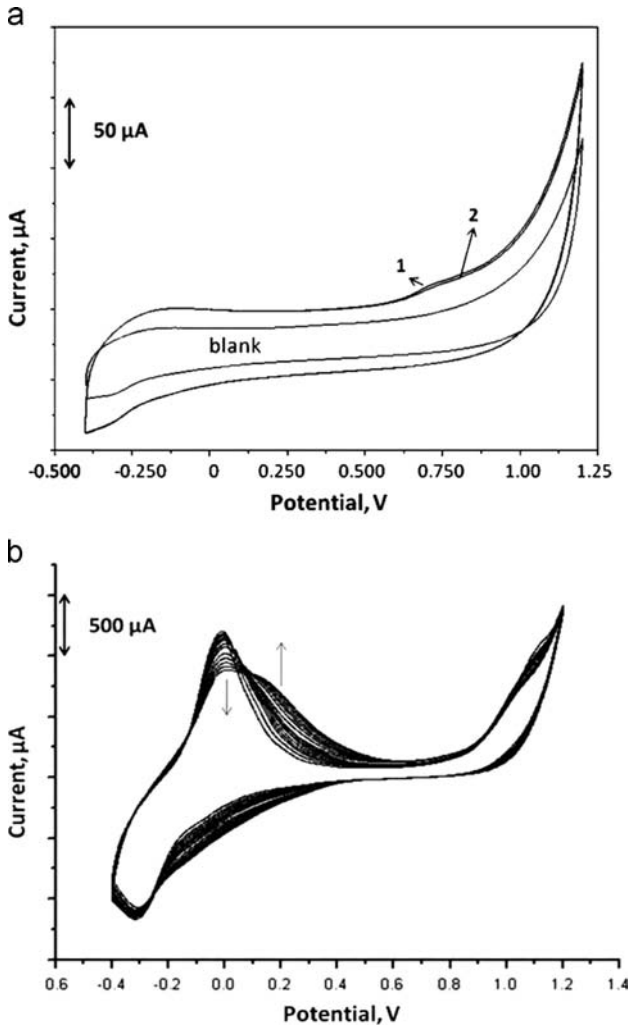

Fig. 1. Cyclic voltammograms of (a) 8.0×10^{-5} M IRT on the surface of MWCNT modified GCE in 0.04 M BR buffer at pH 10.0 (1: first and 2: second cycles) and (b) electropolymerization of 0.1 mM MB on the surface of MWCNT modified GCE in 0.1 M PBS at pH 7.0, scan rate 100 mV s^{-1}.

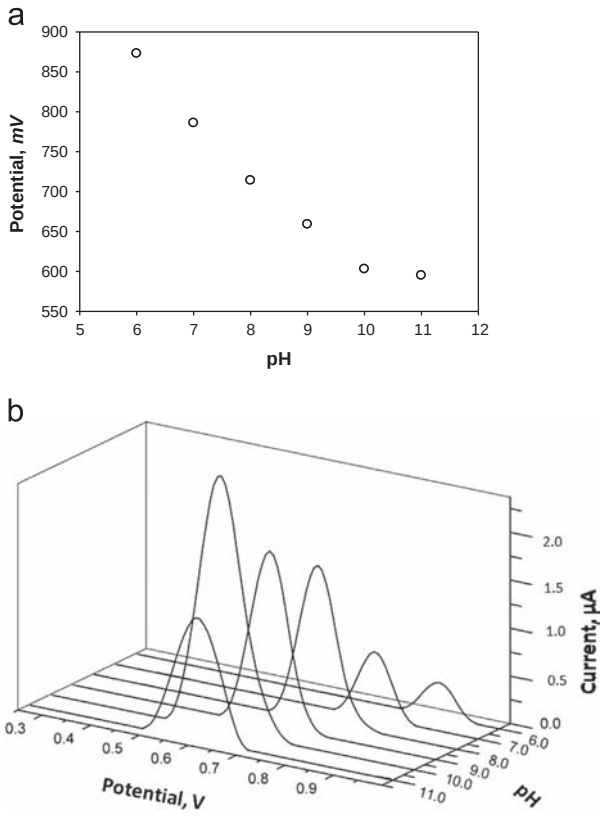

Fig. 2. (a) Effect of pH on 8.0×10^{-5} M IRT anodic peak potential (o) BR buffer. (b) Differential pulse voltammograms of 8.0×10^{-5} M IRT on the surface of PMB/MWCNT modified GCE in various pHs of buffer solution between pH 6.0 and 11.0 at 20 mV s^{-1}.

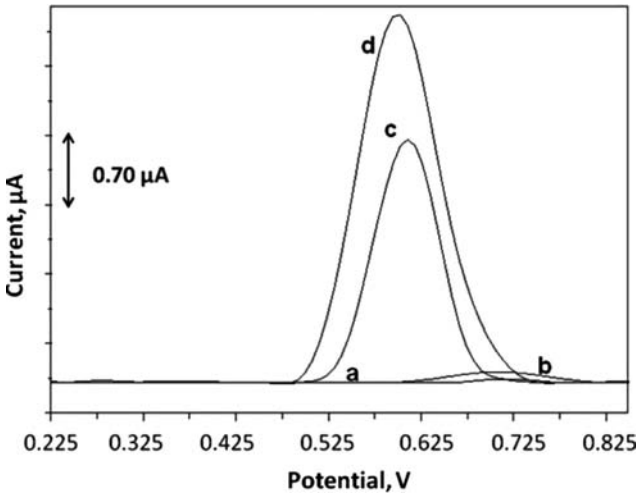

Fig. 3. Differential pulse voltammograms of 8.0×10^{-5} M IRT on the surface of various electrodes. (a) Bare GCE, (b) PMB modified GCE, (c) MWCNT modified GCE, and (d) PMB/MWCNT modified GCE at 20 mV s^{-1} scan rate in 0.04 M BR buffer solution of pH 10.0.

A slope value that is close to the theoritical value of 59 mV/pH indicates that the oxidation peak involves the same number of electrons and protons [44,45]. The width at half height of IRT oxidation peak is $W_{1/2}$~103 mV, close to the theoretical value of 90 mV for an electrochemical reaction involving the transfer of one electron.

The relationship between pH and the peak current of IRT was also investigated. The maximum peak current and the best peak shape were found at pH 10.0 for the sensitive determination of IRT (Fig. 2b).

As seen in Fig. 3, the DP voltammograms of 8×10^{-5} M IRT were shown at PMB/MWCNT-modified GCE, MWCNT-modified GCE, PMB-modified GCE and bare GCE. IRT exhibited only a small oxidation peak current (0.077 µA) at the bare GCE with a high oxidation peak potential at 706 mV. Modified GCE with MWCNT caused less positive oxidation potential to 611 mV and increased peak currents to 1.69 µA. At the PMB/MWCNT-modified GCE, the highest electrochemical activity of IRT was observed with an oxidation peak current of 2.67 µA, which demonstrated a synergy between PMB and MWCNT. MWCNT has a high surface area. This property helps more IRT molecules to be adsorbed or penetrate through the conductive porous channels of PMB. Also, the oxidation potential is lowered due to the electrocatalytic effect of PMB/MWCNT-modified GCE towards IRT oxidation.

3.2. Effect of film thickness

The MWCNT modified GCE was prepared as described in Section 2.4. The electro-deposition of the MB layer on the surface of MWCNT modified GCE was produced by potential cycling between −0.4 V and 1.2 V with 20 cycles. As seen in Fig. 1, the electrochemical signal of PMB film was increased up to the 15 cycles. After the 15 cycles the PMB signal was decreased. On the other hand, by increasing the thickness of the polymer film, the capacitive background current is increased, which worsened the detection limit of the voltammetric measurements. This observation suggests that the polymer layer with high thickness makes the electrode surface passive. Thus, polymer-coated electrode with 15 cycles of potential was chosen as the modified electrode for all voltammetric analysis (Fig. 1). Therefore, the GCE coated with a layer-by-layer of 10 µL MWCNT and 15 cycles deposition of PMB was used as optimum conditions for the preparation of the modified electrode.

The areas of the PMB/MWCNT-modified GCE and the bare GCE were obtained by CV using 1 mmol L^{-1} $K_3Fe(CN)_6$, $n=1$, and $D_R=7.6\times10^{-6}$ cm s^{-1} (0.1 M KCl). Then from the slope of the current density − scan rate ($I_{pa}-\upsilon^{1/2}$) relation, the microscopic areas were calculated as 0.669 cm^2 for bare GCE and 1.448 cm^2 for modified GCE. The surface area of modified GCE was found 2.16 times bigger than the bare GCE.

3.3. Effect of scan rate

The effect of potential scan rate was also investigated in a solution containing 8.0×10^{-5} M IRT with pH 10.0. The oxidation process is diffusion-controlled as deduced from the linear dependence of the anodic peak current (I_{pa}) on the square root of the potential scan rate ($\upsilon^{1/2}$) over a wide range of potential scan rates (from 5 to 500 mV/s).

$$I_p(\mu A)=0.212\,\upsilon^{1/2}+0.455 (r=0.994)$$

$$\log(Ip)=0.348\ \log \upsilon – 0.272 (r=0.978)$$

The slope of log *I*p versus log υ was close to 0.5, indicating the reaction is diffusion-controlled.

A relationship between peak potential, *E*p and logarithm of scan rate, υ can be expressed by the following equation:

$$Ep\ (V)=0.806+0.0824\ \log \upsilon\ (V/s) (r=0.998)$$

For a totally irreversible electrode process, *E*p and υ are defined by the following equation:

$$E_p=E^{0'}+(2.303RT/\alpha nF)\log(RTk^0/\alpha nF)+(2.303RT/\alpha nF)\log \upsilon$$

where k^0 is standard heteregenous rate constant, $E^{0'}$ is formal potential, α is transfer coefficient of the oxidation of IRT and n_α is the number of the electron transfer in the rate-determination step, D_R is diffusion coefficient of IRT. F, R, T symbols have their usual significance. α is generally assumed as 0.5 in the totally irreversible electrode process [46]. From the slope of the *E*p versus logarithm of scan rate (log υ) plot, the number of electron transfer was calculated as 1.43. Therefore, the oxidation of IRT reaction needed one-electron transfer process.

3.4. Controlled potential coulometry

Controlled potential coulometry was performed to obtain the number of electrons transferred. The transferred electron numbers were calculated from the charge consumed of the low concentration of IRT. The total charge 334 mC consumed for the electrolysis of IRT and substituted into Faraday's equation; $Q=nFN$, where *Q* is the total charge consumed for the electrolysis, *N* is the number of molar equivalents, *F* is the Faraday constant (96,500 C). By using Faraday equation, the number of electrons transferred was calculated. 4×10^{-6} M IRT solution was purged with nitrogen. During the electrolysis, solution was stirred continously. The number of transferred electron was obtained as 1 according to the coulometric measurements.

3.5. Surface characterization of the modified electrode

The morphology of the modifier PMB and MWCNT films on the GCE surface was analyzed by SEM with 2 µm bar scale. Fig. 4 shows the significant surface morphology differences between bare GCE, MWCNT-modified GCE, PMB-modified GCE and PMB/MWCNT-modified GCE. All images were obtained at 20,000×. The GCE surface with MWCNT was highly dispersed, uniformly coated, and was found similar to the previous findings [47]. As seen in Fig. 4, PMB covered the MWCNT on the GCE surface and formed composite film.

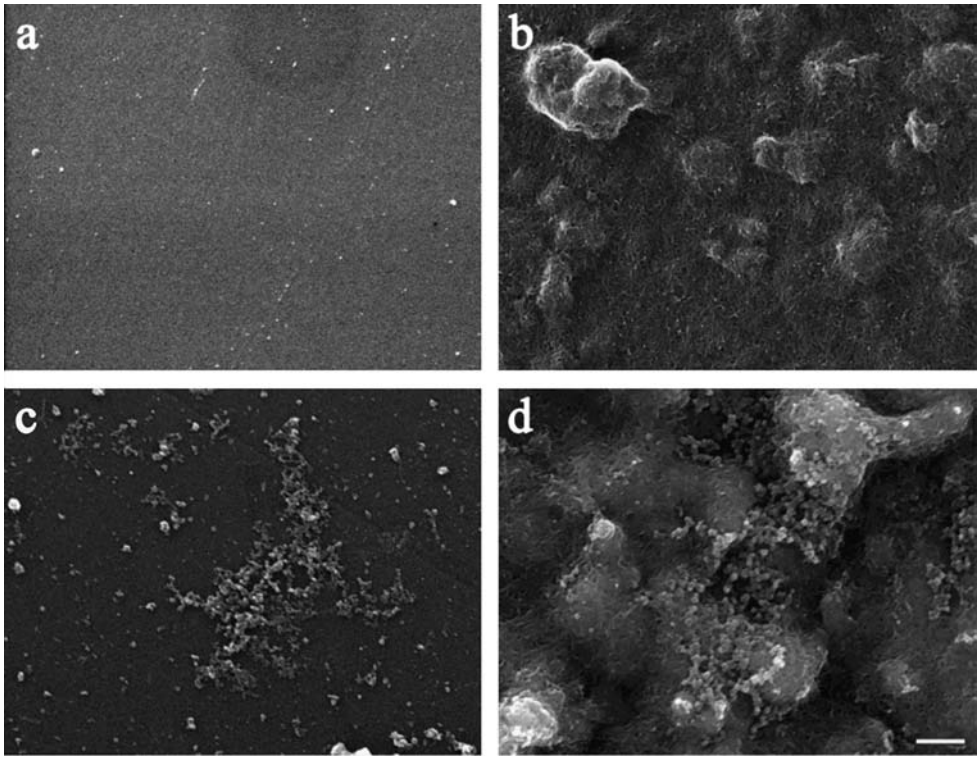

Fig. 4. Surface morphology of bare GCE (a) MWCNT modified GCE, (b) PMB modified GCE, (c) PMB/MWCNT modified GCE, and (d) obtained by SEM. Scale bar = 2 μm. Electrodes were initially coated with AuPd in 15 nm thickness using sputter coater and wieved at 20 keV, 20,000 ×.

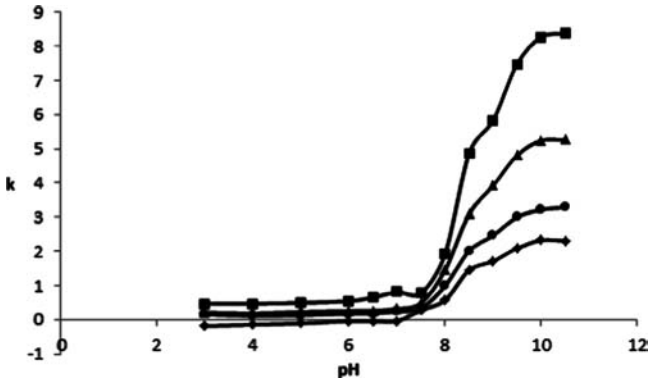

Fig. 5. Plot of chromatographic retention factor, k, vs. the pH of mobile phase; 35% (v/v) ACN–water: ■, 40% (v/v) ACN–water: ▲, 45% (v/v) ACN–water: ●, and 50% (v/v) ACN–water: ◆.

3.6. Determination of dissociation constant (pK_a)

Cyclic voltammetric measurement showed an irreversible nature of the oxidation process at pH 10.0 BR buffer (Fig. 1a). The scanning was started at −0.250 V in the positive direction, the anodic oxidation of IRT was observed at 0.750 V on GCE. Reduction signal did not occur on cathodic part (later than +1.20 V). DPVof IRT exhibited a well defined anodic peak at different potential values depending on pH values, supporting electrolyte composition and electrode material (Fig. 2b). Thus the observed pH dependence indicates that the electroactive group which is corresponding to the IRT main oxidation peak is in acid–base equilibrium with pK_a about 10.0. Above pH 10.0 the peak potential nearly becomes pH independent (Fig. 2a). This can be associated with the pK_a of IRT that was found as 9.3 (±0.20) using ACD Lab. This break could be due to a change in protonation–deprotonation process of electroactive molecule. The pH-independent zone above pH 10.0 means that there are no proton transfer steps before the electron transfer rate determining step. Since, no dissociation occurs before the electron transfer rate-determining step, the oxidation potential remains pH independent for GCE. The pK_a value of IRT was investigated with the RP-LC method. The retention factors were determined for each mobile phase composition and studied pH values. For this purpose, the effect of mobile phase pH on the retention factors was investigated. pK_a, K_{BH^+}, and K_B values of these compounds were calculated by using the software NLREG 4.0 from k/pH data [34]. The dependence of the retention factors on the pH value of the mobile phase (between 35 and 50% v/v) are given in Fig. 5. The obtained values of retention factors for the neutral and ionic forms of IRT in 35–50% (v/v) acetonitrile calculated by NLREG program in several ACN:water mixtures are given in Table 1.

Table 1
Presently obtained and previously-reported pK_a values and capacity factors of IRT.

	NLREG pK_a	K_{BH^+}	K_B
35% ACN	8.5 ± 0.06	0.47 ± 0.12	8.4 ± 0.21
40% ACN	8.5 ± 0.04	0.18 ± 0.05	5.3 ± 0.08
45% ACN	8.4 ± 0.04	0.12 ± 0.04	3.3 ± 0.06
50% ACN	8.4 ± 0.08	0.11 ± 0.05	2.3 ± 0.08
Literature values	8.7 ± 0.09[41] (in water)		
Yasuda-Shed	8.8		
ACD LAB	9.3 ± 0.20		

Aqueous dissociation constant was required for routine analysis. For this reason, the aqueous pK_a value of IRT was determined by Yasuda–Shedlovsky equation [14].

$$pK_a + \log[H_2O] = a_\varepsilon \varepsilon^{-1} + b_\varepsilon \quad (3)$$

Table 1 also gives the pK_a values obtained from Yasuda–Shedlovsky equation, reported in the literature [48], together with those predicted by the program ACD Lab [15].

Table 2
Regression data of the calibration lines for quantitative determination of IRT by DPV and RP-LC method.

	Modified GCE	RP-LC
Measured potential (V)/retention time (min)	0.60	5.2
Linearity range (M)	8.0×10^{-6}–8.0×10^{-5}	8.0×10^{-7}–1.9×10^{-5}
Slope ($\times10^{4}$)	3.8	75
Intercept	−0.29	0.096
Correlation coefficient	0.998	0.999
S.E. of slope ($\times10^{3}$)	1.3	9.5
S.E. of intercept ($\times10^{-2}$)	5.7	9.4
LOD ($\times10^{-7}$ M)	2.1	0.46
LOQ ($\times10^{-7}$ M)	6.5	1.4
Repeatability of peak current/peak area (R.S.D.%)[a]	0.71	0.15
Repeatability of peak potential/retention time (R.S.D.%)[a]	0.59	0.41
Reproducibility of peak current/peak area (R.S.D.%)[a]	0.94	0.20
Reproducibility of peak potential/retention time (R.S.D.%)[a]	0.59	0.26

[a] Obtained from five experiments.

The pK_a value of IRT (belonging to the protonation of the tertiary amine) decreased with increasing the organic modifier percentage in the mobile phase. There are 3 main effects that cause the change of the pK_a values with added organic solvents: variation of the acid/base properties of the solvent, variation of the dielectric constant of the medium which affects electrostatic interactions between ions, and variation of the specific solute/solvent interactions (e.g., hydrogen bonding).

3.7. Validation of the analytical methods

For analytical purposes, best response in relation to the peak current sensitivity and reproducibility was obtained in 0.04 M BR buffer solution at pH 10.0.

The calibration curve for the IRT electrochemical reaction at the PMB/MWCNT-modified GCE was characterized under the selected experimental conditions using DPV technique. The anodic peak current increased linearly with IRT concentration ranging from 8.0×10^{-6} to 8.0×10^{-5} M. The detection limit of IRT was calculated as 2.14×10^{-7} M. The characteristics of the calibration lines and their related validation parameters are summarized in Table 2. The repeatability and reproducibility of the PMB/MWCNT modified GCE were also examined in within day and between days. More significant reproducibility (robustness) was also obtained between each renewed modified electrodes. The electrode-to-electrode reproducibility of the proposed method was also examined on five PMB/MWCNT modified GCE constructed individually and the RSD of the five average peak currents of 1.72%.

The LOD and LOQ parameters were calculated according to the 3 s/m and 10 s/m criterions, respectively, where s is the standard deviation of the peak currents (five measurements) and m is the slope of related calibrating graph [49].

The low value of standard error (SE) of slope and intercept, LOD and LOQ values indicated good sensitivity and applicability. The precision of the technique was calculated from five replicate experiments in different solutions having the same concentration of IRT within the same day using DPV at the PMB/MWCNT modified GCE.

The efficiency of the developed method was evaluated by the quantity of IRT in injectable dosage form (labeled value 100 mg/5 ml). The concentration of IRT determined in this solution using the DPV method is reported in Table 3.

For checking the accuracy, precision and selectivity of the electroanalytical technique and in order to know whether the excipients in injectable dosage form show any interference with the analysis, the recovery studies were evaluated after addition of known amounts of IRT. Recovery studies showed absence of interference from commonly used pharmaceutical dosage form presented its excipients and proved that the proposed methods had adequate precision and accuracy (Table 3).

Table 3
The results of the determination of IRT from dosage form and recovery experiments achieved by the DPV and RP-LC method.

	Modified GCE	RP-LC
Labeled claim (mg/5 mL)	100.00	100.00
Amount found[a] (mg/5 mL)	100.15	100.08
R.S.D.%	0.21	0.18
Bias %	−0.15	−0.08
t_{value}	0.480	$t_{theoretical}$: 2.31
F_{value}	0.293	$F_{theoretical}$: 2.60
Added (mg)	100.00	100.00
Found[a] (mg)	100.45	100.10
Average recovered (%)	100.46	100.09
R.S.D.% of recovery	0.45	0.09
Bias %	−0.45	−0.10

[a] Obtained from five experiments.

For RP-LC analysis, the influence of pH of the mobile phase and column temperature were examined in order to optimize the chromatographic conditions for RP-LC determination of IRT. pH 8.0 was selected as optimum value with best peak asymmetry and retention values. pH of the mobile phase has always been adjusted with 20 mM orthophosphoric acid. The column temperature was set to 25 °C. Finally, the mobile phase ACN:water 40:60 (v/v) with 20 mM H_3PO_4 (at pH 8.0) at a flow rate of 1.0 mL min^{-1} was found to be the most suitable carrier for RP-LC analysis.

After determining the optimum conditions, a satisfactory resolution was obtained in a short analysis time (6 min. Fig. 6). Sharp and symmetrical well-resolved peaks were obtained for all compounds. 220 and 320 nm wavelengths were selected for IRT and IS detection, respectively.

System suitability tests are used to verify that reproducibility of the chromatographic system which is adequate for the analysis to be done. Some of the tests were carried out on freshly prepared standard solutions. Tailing factors of 1.38 and 1.21 were obtained for IRT and IS, respectively. The theoretical plate numbers (N) were 4559 for IRT and 5973 for IS. The selectivity factor was 1.76. The chromatographic conditions described ensured adequate retention for IS and IRT. The retention times of IRT and IS were 5.24 and 4.03 min, respectively. The calibration equation used for IRT analysis and LOD, LOQ values were given in Table 3. The adequacy of the developed methods was evaluated by quantifying IRT in

injectable dosage forms. Developed RP-LC methods can be used for the assay of IRT without prior separation of the excipients. The concentration of IRT determined in injectable dosage form using the electroanalytical and RP-LC methods is reported in Table 2. The results showed that the developed methods could be applied to IRT assay in injectable dosage form without any interference (Table 2).

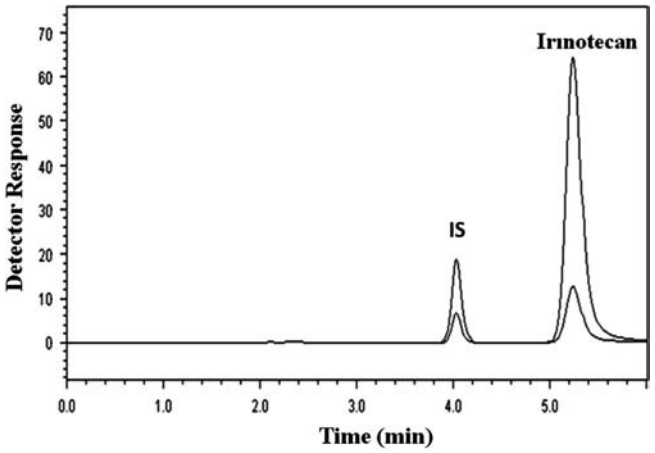

Fig. 6. Chromatogram of standard mixture: IS (8.09×10^{-6} M) and IRT (1.28×10^{-5} M), ACN:water 40:60 (v/v) with 20 mM H_3PO_4 (at pH 8.0) at a flow rate of 1.0 mL/min. 220 and 320 nm wavelengths were selected for IRT and IS detection, respectively.

The performance of the developed RP-LC and DPV methods was checked and compared between each other using Student's *t*- and *F*-tests at 95% of the confidence level. Hence, the accuracy and precision of the methods can be compared. As a result of experimental calculations, the calculated Student-*t* and *F*-tests results were less than that of theoretical *t*- and *F* values. It means that there were no significant differences between the performances of RP-LC and DPV methods.

3.8. Specificity and stress-degradation studies

Stress testing of the drug substance can help to identify the possible degradation products, which can in turn help establishing the degradation pathways and the intrinsic stability of the molecule. The results of stress testing studies indicated a high degree of specificity of this method for IRT compound. The chromatograms of drug, after being submitted to different degradation conditions are given in Fig. 7.

IRT was completely degraded under acid hydrolysis and alkaline solutions. Degradation studies showed that IRT is more stable than the other stress conditions when heated (100 °C for 6 h) or exposed to UV light.

Table 4 shows the results of the forced degradation studies using the developed method, indicating degradation percentage and purity of drug peak in the chromatograms.

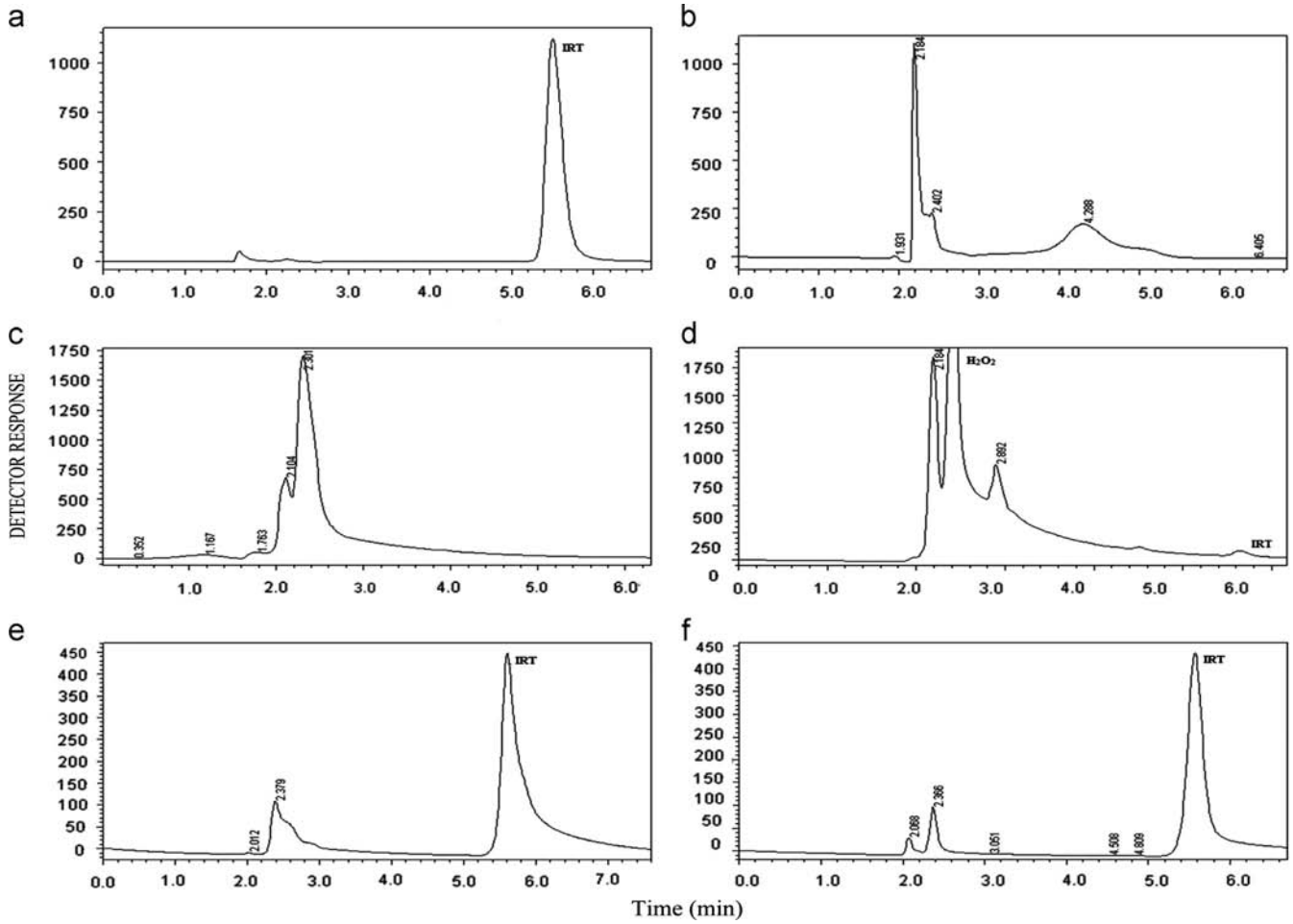

Fig. 7. Typical LC chromatograms of drugs under drastic stressed conditions: (a) 1.61×10^{-4} M IRT, (b) 1.0 M HCl at 80 °C after 30 min, (c) 1.0 M NaOH at 80 °C after 30 min, (d) H_2O_2 3% at 75 °C after 30 min, (e) in UV light (254 nm) after 24 h, and (f) at 100 °C after 6 h.

Table 4
The RP-LC results of hydrolytic, oxidizing, thermal and photolytic stress conditions of drug.

The response of stress conditions	Degradation of IRT (%)
HCl (1.0 M)	100.00
NaOH (1.0 M)	100.00
H_2O_2 (3%)	96.34
UV (24 h)	52.41
Heating (100 °C 6 h)	51.37

4. Conclusion

In this study, the polyMB/MWCNT-modified GCE has been developed for sensitive electrochemical detection of IRT. Compared with bare GCE with the PMB/MWCNT-modified GCE, the modified electrode exhibits a shift to the lower oxidation potential of IRT due to the electrocatalytic effect and a significant increase of the peak current. SEM results have confirmed with the enhancement of surface structure with the composite film modified electrode. The proposed method for IRT on the PMB/MWCNT-modified GCE has been applied to the pharmaceutical dosage forms.

The pK_a value of IRT was determined by the electroanalytical and RP-LC methods. Similar pK_a value of IRT was obtained with both methods. The developed RP-LC method has been applied for comparing method and this LC work also presents novel results regarding with the determination of pK_a value of IRT. Also, the validated RP-LC method has the advantage of simplicity, precision, rapidity and reliability. The results of stress testing undertaken according to the ICH Guidelines reveal that the method is selective and stability-indicating. The proposed RP-LC method has the ability to separate IRT from their degradation products and related substances.

References

[1] D.F. Chollet, L. Goumaz, A. Renard, J. Chromatogr. B 718 (1998) 163–175.
[2] J.J. Hwang, J.L. Marshall, N. Rizvi, Oncology 17 (2003) S46–S51.
[3] R. Haijan, T.G. Huat, Chin. J. Chem. 30 (2012) 738–742.
[4] V. Murali Balaram, J. Venkateswara Rao, S. Ramakrishnag, G. Sankar Ganesh, T. Balamurali Krishna, E. J. Chem. 4 (2007) 128–136.
[5] V. Kiran Kumar, N. Appala Raju, N. Rani, J.V.L.N. Seshagiri Rao, T. Satyanarayana, Asian J. Res. Chem. 2 (2009) 54–56.
[6] A. Mohammadi, F. Esmaeili, R. Dinarvand, F. Atyabi, R.B. Walker, Asian J. Chem. 22 (2010) 3966–3972.
[7] Z.P. Hu, X.X. Yang, X. Chen, E. Chan, W. Duan, S.F. Zhou, J. Chromatogr. B 850 (2007) 575–580.
[8] M.T. Baylatry, A.C. Joly, J.P. Pelage, L. Bengrine-Lefevre, J.L. Prugnaud, A. Laurent, C. Fernandez, J. Chromatogr. B 878 (2010) 738–742.
[9] X. Yang, Z. Hu, S.Y. Chan, B.C. Goh, W. Duan, E. Chan, S. Zhou, J. Chromatogr. B 821 (2005) 221–228.
[10] N. Sanli, G. Fonrodona, D. Barron, G. Ozkan, J. Barbosa, J. Chromatogr. A 975 (2002) 299–309.
[11] M. Gumustas, S. Sanli, N. Sanli, S.A. Ozkan, Talanta 82 (2010) 1528–1537.
[12] N. Sanli, S. Sanli, U. Sızır, M. Gumustas, S.A. Ozkan, Chromatographia 73 (2011) 1171–1176.
[13] N. Karadas, S. Sanli, M. Gumustas, S.A. Ozkan, J. Pharm. Biomed. Anal. 66 (2012) 116–125.
[14] T. Shedlovsky, in: B. Peasce (Ed.), Electrolytes, Pergamon Press, New York, 1962.
[15] ACD/pKa dB, version 6.09, Advanced Chemistry Development, Inc., Toronto ON, Canada, 2002. ⟨www.acdlabs.com⟩.
[16] C.P. Andrieux, O. Haas, J.M. Saveant, J. Am. Chem. Soc. 108 (1986) 8175–8182.
[17] E.W. Wong, P.E. Sheehan, C.M. Lieber, Science 277 (1997) 1971–1975.
[18] J. Riu, A. Maroto, F.X. Rius, Talanta 69 (2006) 288–301.
[19] J.W. Mintmire, B.I. Dunlap, C.T. White, Phys. Rev. Lett. 68 (1992) 631–634.
[20] J. Liu, A.G. Rinzler, H.J. Dai, J.H. Hafner, R.K. Bradley, P.J. Boul, A. Lu, T. Iverson, K. Shelimov, C.B. Huffman, F. Rodriguez-Macias, Y.S. Shon, T.R. Lee, D.T. Colbert, R.E. Smalley, Science 280 (1998) 1253–1256.
[21] R.H. Baughman, C.X. Cui, A.A. Zakhidov, Z. Iqbal, J.N. Barisci, G.M. Spinks, G.G. Wallace, A. Mazzoldi, D. De Rossi, A.G. Rinzler, O. Jaschinski, S. Roth, M. Kertesz, Science 284 (1999) 1340–1344.
[22] L. Kavan, L. Dunsch, H. Kataura, Carbon 42 (2004) 1011–1019.
[23] M.E. Ghica, R. Pauliukaite, O. Fatibello-Filho, C.M.A. Brett, Sens. Actuators B 142 (2009) 308–315.
[24] R. Pauliukaite, M.E. Ghica, O. Fatibello-Filho, C.M.A. Brett, Anal. Chem. 81 (2009) 5364–5372.
[25] I. Becerik, F. Kadirgan, Synth. Met. 124 (2001) 379–384.
[26] A.A. Karyakin, E.E. Karyakina, H.L. Schmidt, Electroanalysis 11 (1999) 149–155.
[27] K. Tanaka, S. Ikeda, N. Oyama, K. Tokuda, T. Ohsaka, Anal. Sci. 9 (1993) 783–789.
[28] P. Gajendran, R. Saraswathi, Pure Appl. Chem. 80 (2008) 2377–2395.
[29] E. Mendoza, J. Orozco, C. Jiménez-Jorquera, A.B. Gonzalez-Guerrero, A. Calle, L.M. Lechuga, C. Fernandez-Sánchez, Nanotechnology 19 (2008) 1–6.
[30] J. Wang, J. Dai, T. Yarlagadda, Langmuir 21 (2005) 9–12.
[31] ICH, Stability Testing of New Drug Substances and Products (Q1AR) International Conference on Harmonization IFPMA, Geneva, 2000.
[32] J. Ermer, in: J.H McB. Miller (Ed.), Method Validation in Pharmaceutical Analysis, Wiley-VCH Publ, Weinheim, 2005.
[33] ICH, Topic Q2A Validation of Analytical Procedures, Methodology, PMP/ICH/281/95.
[34] P.H. Sherrod, NLREG Version 4.0, The United States Pharmacopoeial Convention, Inc., ⟨http://www.sandh.com/Sherrod⟩.
[35] C.M. Riley, T.W. Rosanske (Eds.), Development and Validation of Analytical Methods, Elsevier Science Ltd., New York, 1996.
[36] P. De Bievre, H. Günzler (Eds.), Validation in Chemical Measurements, Springer Publisher, Berlin, 2005.
[37] I.R. Berry, D. Harpaz, Validation of Active Pharmaceutical Ingredients, second ed., CRC Press, Washington, 2001.
[38] R.C. Pena, M. Bertotti, C.M.A. Brett, Electroanal 23 (2011) 2290–2296.
[39] A. Golcu, B. Dogan, S.A. Ozkan, Anal. Lett. 38 (2005) 1913–1931.
[40] A. Alvarez-Luece, L. Naranjo, L.J. Nunez-Vergara, J.A. Squella, J. Pharm. Biomed. Anal. 16 (1998) 853–862.
[41] J. Zhao, Y. Zhang, K. Wu, J. Chen, Y. Zhaou, Food Chem. 128 (2011) 569–572.
[42] J. Grimshaw, Electrochemical reactions and mechanism in organic chemistry, first ed., Elsevier Publishers, Amsterdam, 2000.
[43] H. Lund, O. Hammerich, Organic Electrochemistry, fourth ed., Marcel Dekker, New York, 2001.
[44] M.E. Ghica, C.M.A. Brett, J. Electroanal. Chem. 629 (2009) 35–42.
[45] M.S. Maio Quintino, M. Yamashita, L. Angnes, Electroanalysis 18 (2006) 655–661.
[46] K.B. Wu, Y.Y. Sun, S.H. Hu, Sens. Actuators B 96 (2003) 658–662.
[47] K.Y. Chun, S.K. Choi, H.J. Kong, C.Y. Park, C.J. Lee, Carbon 44 (2006) 1491–1495.
[48] N. Sanli, S. Sanlı, G. Alsancak, J. Chem. Eng. Data 55 (2010) 2695–2699.
[49] S.A. Ozkan (Ed.), Electroanalytical Methods in Pharmaceutical Analysis and their Validation, HNB Publishing, New York, 2012.